Demixing/Mixing of Polystyrene with Poly(methylphenylsiloxane) in a Two-Step Cooling/Heating Process: Jump Spinodal Specification Method

M. Graca,[†] S. A. Wieczorek,*[,†] M. Fiałkowski,[†] and R. Hołyst[†,‡,§]

Institute of Physical Chemistry, Polish Academy of Sciences, Kasprzaka 44/52, 01-224 Warsaw, Poland; Department of Mathematics and Natural Sciences−College of Science, Cardinal Stefan Wyszyński University, Dewajtis 5, 01-815 Warsaw, Poland; and Ecole Normale Superieure, Labo de Physique, 46 Allee d'Italie, Lyon, France

Received March 28, 2002

ABSTRACT: We present experimental studies of the mixing process of a homopolymer blend of poly(methylphenylsiloxane) (PMPS) with polystyrene (PS). The system is first allowed to decompose spinodally at low temperature for few minutes and next is heated to a higher temperature to the one-phase or two-phase (metastable or unstable) region. In all cases the intensity drops initially after the temperature jump. In the one-phase region the intensity drops to the base scattering. In the metastable region it drops initially, and later on it starts to grow. In this region the peak position shifts strongly toward small wavevectors, and the intensity drops considerably. Finally, in the spinodal (unstable) region the peak position shifts toward smaller wavevectors, but the intensity of the peak hardly changes before increasing again. The decrease of the peak intensity is exponential with the characteristic decay time which approaches infinity when the temperature of the jump approaches that of the quench. The mixing process mainly involves the interdiffusion of polymers, without global movement of the interface. Small domains disappear faster than larger domains, and therefore the peak position (indicating an average size of the domains) shifts toward smaller wavevectors. In the metastable region the average wavevector as a function of time has a characteristic minimum, which shifts toward zero as we approach the spinodal. If the jump is made to the unstable region, the average wavevector monotonically decreases with time. The average wavevector, after temperature jump, allows to predict the location of the binodal and spinodal. We call this new method of spinodal location a jump spinodal specification method (JSS method). The generic features of this method have been confirmed in the computer simulations of the Flory−Huggins−de Gennes model with the Langevin dynamics for the mixture of polybutadiene and deuterated polybutadiene.

1. Introduction

Homopolymer mixtures are far from being ideal, and consequently at suitable conditions we can expect demixing in the liquid state. The demixing process has been very thoroughly studied in homopolymer blends during the past two decades.[1−17] There is also a vast literature concerning a theoretical approach to the general aspects of the kinetics of phase separation or ordering.[1,3,17−20] On the contrary, the reversed process of mixing received much less attention.[21−28] Both processes are important from the technological point of view since many modern materials are composed of several polymeric components which in the process of preparation of the material are mixed in a liquid state before being quenched below the glass temperature.

The process of the phase separation (demixing) is usually studied by considering a homogeneous homopolymer blend (AB) which is quenched below the consolute (critical temperature) into the thermodynamically unstable region (spinodal region) of the phase diagram. In this case, the spinodal decomposition (SD) takes place, which manifests in the spontaneous growth of the concentration fluctuations that leads the system from the homogeneous to the two-phase state. Shortly after the phase separation starts the domains of A and B component are formed, and the interface between the two phases can be specified. There are actually few different regimes of the separation processes (at least early, intermediate, and late) studied and described in detail by Bates[4] and Hashimoto[9] for homopolymer blends.

Early stages of the spinodal decomposition process are described by the linearized Cahn−Hilliard theory.[18−20] After the temperature quench below the spinodal temperature, the system becomes unstable with respect to small fluctuations of wavevector q smaller than some value q_0. The key prediction of the theory is the exponential growth of the scattering intensity $S(q,t)$ in time with a well-defined maximum at $q_{max} = q_0/\sqrt{2}$. Interpenetrating A-rich and B-rich domains of the size of $1/q_{max}$ form a bicontinuous structure. At this point the domains mainly saturate; i.e., the scattering is mainly due to the increase in the composition difference between A-rich and B-rich domains. Once the composition inside A-rich and B-rich domains gets saturated, the further coarsening processes (growth of the average domain size, $L(t)$ in time t) is driven by the interface curvature.[20] The system at long times gets finally into the late stage growth regime. In the late regime, one finds a power law growth of $L(t)$ and scaling; i.e., a morphological pattern of the domains at earlier times looks statistically similar to a pattern at later times apart from the global change of scale implied by the growth of $L(t)$—the domain size. Quantitatively, it means for example that the correlation function of the homopolymer concentration has the following functional

[†] Polish Academy of Sciences.
[‡] Cardinal Stefan Wyszyński University.
[§] Ecole Normale Superieure, Labo de Physique.

10.1021/ma020499c CCC: $22.00
Published on Web 10/19/2002

form:

$$g(\mathbf{r},t) = g(\mathbf{r}/L(t)) \tag{1}$$

where

$$L(t) \sim t^{\beta} \tag{2}$$

the characteristic length scale in the system, scales algebraically with time t with the exponent β depending on the particular dynamic process (i.e., diffusion $\beta = {}^1/_3$, hydrodynamic flow $\beta = 1$, etc.) which governs coarsening.[20] The Fourier transform of the correlation function gives the scattering intensity and can be represented in the following scaling form:

$$S(q,t) = L^3(t)Y[qL(t)] \tag{3}$$

where q is the scattering wavevector and Y is the scaling function. In general, one uses relation 3 to check the scaling. In practice,[9,11] one determines the location of the maximum of $S(q,t)$, $q_{max} \sim 1/L(t)$, and the value of $S(q,t)$ at the maximum, S_{max}, to have a quick check of scaling since according to (3)

$$S_{max}(t) \sim q_{max}(t)^{-3} \tag{4}$$

If $S_{max} \sim t^{\alpha}$ and $q_{max} \sim t^{-\beta}$, then scaling implies that $\alpha = 3\beta$. In general, when the domains are still not saturated, we expect that approximately

$$S_{max}(t) \sim \langle \phi(t)^2 \rangle \, q_{max}(t)^{-3} \tag{5}$$

where $\langle \phi(t)^2 \rangle$ denotes the composition fluctuations in the domains. Therefore, in principle, one can determine the time scale for the saturation of the domains in the separation process from this formula.

The mixtures, of low viscosity, undergoing spinodal decomposition do not remain for a long time in their unstable early configuration, contrary to the high molecular weights polymer blends. The latter are very viscous liquids, and the whole kinetics of phase separation is very slow, allowing a detailed experimental observation of the process.[3,9] Moreover, the concept of the spinodal which is hardly accessible experimentally for low molecular weight mixtures is valid for high molecular weight polymers, where the limit of kinetic stability in the metastable region coincides with the spinodal.[3] Also, the analysis of the early stages of spinodal decomposition shows that for polymers it is experimentally relevant. In a metastable region (between the spinodal and binodal), the process of phase separation starts via nucleation of a critical nucleus of one phase. The size of the critical nucleus tends to zero at the spinodal and to infinity at the binodal. A typical size of the critical nucleus (far from the spinodal or binodal) is about few correlation lengths and would not be much larger than 10 times the radius of gyration.

As we have mentioned, the demixing processes is fairly well understood. On the other hand, only recently the reversed process of mixing has started to be studied.[21−28] Here our main interest is to observe mixing in an AB homopolymer blend which is initially prepared in a nonuniform liquid state. The initial state is obtained via spinodal decomposition. First, we quench the system below the spinodal, wait a certain time in order to have a nonuniform state, and next heat the system observing the pathway of the mixing process, i.e., transformation of the nonuniform state into the uniform one. In this paper we concentrate on the nonuniform states obtained in the intermediate stages of spinodal decomposition. In all the previous papers, the authors[21−28] concentrated on the mixing (dissolution) *in a one-phase region*. Here we would like to see how the mixing (or partial mixing) occurs when the system is heated *to the one-phase, metastable, or unstable region*, but above the temperature of the initial quench.

The following questions can be posed: *How fast is the mixing process? Does partial mixing occur when the nonuniform system is heated to metastable or, still, unstable region? What are the morphological changes during mixing? Does the binodal or spinodal affect mixing?*

We will try to find at least partial answers to these questions on the basis of the evolution of the scattering intensity summed over the linear array of photodiodes, defined as

$$\delta = \int S(q,t)\, \mathrm{d}q \tag{6}$$

and the average wavevector q_{av}:

$$q_{av} = \frac{\int qS(q,t)\, \mathrm{d}q}{\int S(q,t)\, \mathrm{d}q} \tag{7}$$

Please note that δ is not the total scattered intensity since we do not integrate in eq 6 with a proper measure q^2 but only sum the intensity over the linear array of photodiodes. We have used this definition for practical purposes, since it is easy to implement in the experiment and was simply used to reduce the noise level on the photodiodes. Instead of q_{av} we could use also q_{max}, but the former is much easier to determine and with a much better accuracy than the latter. Moreover, q_{av} contains information about the general shape of the scattering intensity and q_{max} only about its maximum. Therefore, they may have slightly different behavior, although qualitatively they should behave similarly. Also, $S_{max}(t)$ should behave qualitatively similarly as δ. Quantitatively, in the scaling regime if $q_{max} \sim q_{av} \sim t^{-\beta} \sim 1/L(t)$, then $S_{max} \sim t^{3\beta}$ and $\delta \sim t^{2\beta}$. It is worth mentioning that the data that we get for q_{max} and S_{max} are very noisy in contrast to δ and q_{av}. Nonetheless, we have carefully checked both sets of data from the point of view of their usefulness in the study of the process of mixing.

These quantities are obtained in the light scattering experiments performed on the poly(methylphenylsiloxane)/polystyrene blend. The experiment consists of the following steps: annealing at high temperature in a one-phase region → next a quench below the spinodal → demixing below the spinodal for few minutes → jump to higher temperature and the observation of the mixing (partial mixing) process. In most of the figures we will show the results starting from the quench below the spinodal.

Additionally, we have performed the computer simulations of the binary mixture of polybutadiene-deuterated polybutadiene (hPb/dPb) in order to see whether the obtained results are specific to the polymer mixture used in the experiment or are generic.

2. Experimental Section

We have used a poly(methylphenylsiloxane) (PMPS) from Aldrich Chemical Co. characterized by $M_w = 2274$ and M_w/M_n

= 1.35 and polystyrene (PS) from Fluka Chemical Co., M_w = 10 700 and M_w/M_n = 1.03. PMPS was dried at 70 °C under vacuum and next dissolved with PS in benzene in 60/40% (PS/PMPS) proportions for polymers by weight. Most of the results will be shown for this concetration, but we have additionally studied the 50/50% mixture. Thin films of thickness 50−200 μm were prepared by casting from 20% benzene solution on glass of size 1 cm in diameter. The films were dried at high temperature (70 °C) under vacuum for 1 day and the next 3 days on a hot stage at 130 °C before making the measurements. We have prepared many samples some of them covered with a second glass plate. We could also obtain very flat droplets without a second glass plate. We have observed that a flat droplet gives very little scattering at small scattering angle above the binodal, and only such samples were used for the measurements. Many samples were used since we observed that after 3 days of measurements the chemical composition of the samples starts to change appreciably (probably due to increased oxidation at high temperature), resulting in a change of the binodal temperature. The samples have not degraded at room temperature since for the samples kept at room temperature even after 1 year we could reproduce the last results obtained with that sample 1 year before. For practical purposes a single sample was used for 2 days only, and then it was discarded. The final results are presented for samples of thickness 50 μm covered with a second glass plate. The temperature was controlled up to 0.01 deg, and the typical time for the stabilization of the temperature after a sudden change was 50 s. (This effect was checked experimentally, since for example the average wavevector increases during 50 s when the sample is suddently brought to a lower temperature.) The scattered intensity was detected on a linear array of 512 photodiodes. The measurements were taken every 5 s after the quench and every 0.5 s after the jump. The scattering angles, θ, which are accessible in this experiment are 0.5°−42° and the corresponding wavevectors ($q = 4\pi/\lambda \sin \theta/2$) are 0.2−11 (1/$\mu$m). It means that in the real space we can observe the domains of size $L = 2\pi/q$ between 0.5 and 30 μm (in principle). In practice, the first few photodiodes are too close to the main beam to give reliable results, and therefore in practice the range of L which can be observed in our apparatus is between 0.5 and 5 μm. We use the standard laser (He−Ne, 5 mW) of λ = 632.8 nm and a parabolic mirror to reflect the scattered intensity toward the array of photodiodes. The cloud point measurements gave the location of the binodal at 120 °C ±2 °C. (The large error is due to the chemical degradation of the sample since the cloud point measurements took about a week, and it was repeated for many samples.) The one-phase region is above this temperature. The samples were first annealed at 130 °C and then quenched to temperature 112 °C below the spinodal, where they were allowed to demix for few minutes (5, 8, or 15 min). Some measurements were also performed for 115 °C. Next the samples were heated to higher temperatures, and we observed the decay of the scattering pattern which initially developed at lower temperature.The choice of the time during which we allow the sample to decompose spinodally is dictated by the observation that when we make afterward the temperature jump the peak shifts very quickly toward the small wavevectors. If we keep the sample too long in the unstable region, then after the jump the peak would leave the region of wavevectors accessible in our measurements, and we could not measure its full decay. That is why we kept the sample for a few minutes and not for few hours. However, the phenomena of mixing do not depend qualitatively on this time. We have made additional observations under the optical microscopy when we kept the sample for few hours in the unstable regime and found that the mixing process is qualitatively the same as for the short time observed in the light scattering experiment.

3. Results and Discussion

In Figure 1 we show a schematic picture of the experiment. The binodal and spinodal curves are shown. The system is brought by a temperature quench below the spinodal to temperature T_0 and the temperature jump (to T_1) brings the system back into the one-phase ($T_1 > T_b$), metastable ($T_b > T_1 > T_s$), or unstable region ($T_s > T_1 > T_0$) (but above the initial temperature T_0). Here T_b is the binodal temperature, and T_s is the spinodal temperature for the given volume fraction. We monitor the scattering intensity at T_0 and at T_1. In Figure 2 we show the scattering intensity $S(q,t)$ at various times at the temperature T_0 after the quench from T = 130 °C. We smoothed the noisy data by averaging them over 20 neighbor photodiodes; i.e., each point shown on the plot of $S(q,t)$ vs q has been integrated over the q range corresponding to 20 nearest photodiodes and divided by the range of integration. The range of integration for the points overlapped always for 10 photodiodes; i.e., we made such averaging for 51 photodiodes out of the total number of 512. Another method of averaging consisted in averaging each signal from a photodiode over the five nearest neighbors and keeping all 512 points. We have also checked that the

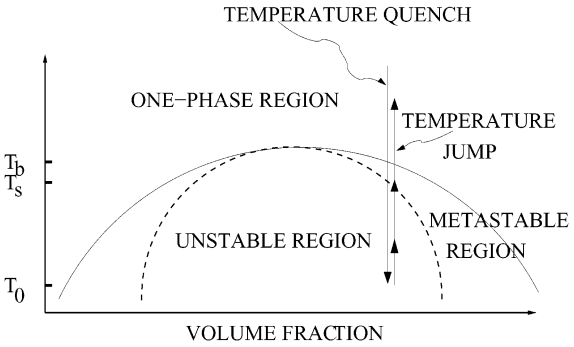

Figure 1. Schematic picture of the general idea of our measurements. The binodal curve is given by the solid line, and the spinodal curve is shown as a dashed line. The system of a fixed volume fraction is quenched from the high temperature to the temperature T_0 below the spinodal (for our volume fraction the spinodal temperature is T_s) and allowed to demix at this temperature for a few minutes. Next it is heated to a higher temperature. Three cases will be discussed: a temperature jump to T_1 in the unstable region $T_0 < T_1 < T_s$, metastable region $T_s < T_1 < T_b$, or a one-phase region $T_1 > T_b$, where T_b denotes the binodal temperature for our volume fraction.

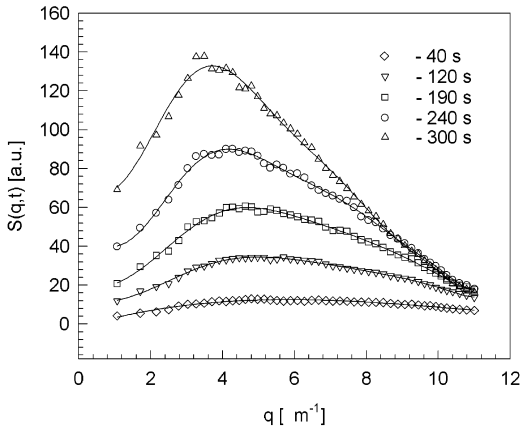

Figure 2. Scattering intensity, $S(q,t)$, after a quench from a high temperature (above the binodal (see Figure 1)) to the temperature T_0 = 112 °C (below the spinodal), as a function of the wavevector q for different times. It shows the known behavior during the spinodal decomposition. The peak grows and its location shifts toward smaller wavevectors, indicating the growth of the average size of the PS-rich and PMPS-rich domains (coarsening process).

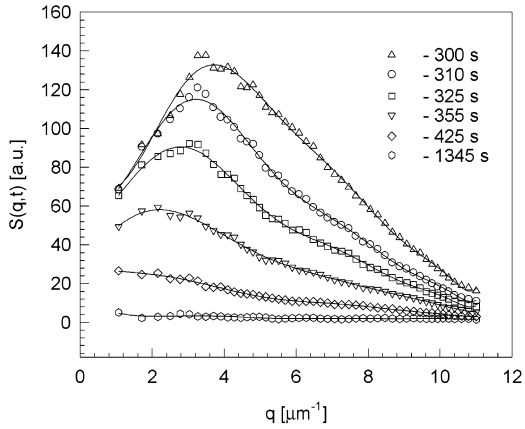

Figure 3. Scattering intensity, $S(q,t)$, after a temperature jump from $T_0 = 112$ °C to the one-phase region $T_1 = 121$ °C above the binodal, as a function of the wavevector q for six times. The peak decreases (indicating the decrease of the saturation of the domains), and its location shifts toward smaller wavevectors, indicating the increase of the average size of the PS-rich and PMPS-rich domains following a global disappearance of small domains (reverse coarsening process) by pure diffusion across domain boundaries.

averaging does not change the results; i.e., both averaging gave the same results.

The standard and well-known result shown in Figure 2 is the increase of the scattering intensity, signaling the spinodal decomposition, and the shift of the peak position toward smaller wavevectors, signaling the process of coarsening. The average size of the domains grows because many small domains formed just after the quench disappear in time, and such coarsening leads to the appearance of bigger domains. The radius of gyration of our polymers is rather small[29] (PMPS, 6.54 Å; PS, 25.4 Å), and therefore we cannot expect to see the Cahn peak. (The wavevector for the Cahn peak is far outside our scale of photodiodes.) Thus, we only observe the evolution of the peak at later times in the intermediate scaling regime. We find that $S_{max} \sim t^{2.76}$, $\delta \sim t^{2.96}$, $q_{max} \sim t^{-0.42}$ (error for the exponents is 0.1), and $q_{av} \sim t^{-0.33}$. It means according to our discussion in the Introduction that the domains are not completely saturated, and the scaling does not work.

A Jump to the One-Phase Region. In Figure 3 we show the behavior of $S(q,t)$ after a temperature jump to the one-phase region. As we can see, the peak position shifts toward smaller wavevectors. At first, the result seems to contradict our intuition since we would expect that the domains should disappear; i.e., their size should decrease in time. To see that after a temperature jump above the spinodal we should observe the shift of the peak position toward the smaller wavevectors, it is sufficient to analyze the Cahn linear theory. We use the Cahn analysis to study the process of the growth of the Cahn peak for time t_0 at temperature T_0 and after a jump to temperature T_1 its evolution for time t. We find, using the standard analysis,[20,21] $S(q,t)$ (in the rescaled dimensionless variables) in the following form:

$$S(q,t) = S(q,0) \exp(2\omega_0(q)t_0) \exp(2\omega_1(q)t) \qquad (8)$$

where $S(q,0)$ is the initial scattering intensity before the quench to T_0, $\omega_0(q) = -q^2(q^2 - {q_0}^2)$ is calculated at T_0, and $\omega_1(q) = -q^2(q^2 + {q_1}^2)$ at T_1, $q_0 \sim 1/(T_s - T_0)$, and $q_1 \sim 1/(T_1 - T_s)$. It follows from eq 8 that the location of the peak is given by

$${q_{max}}^2 = \frac{{q_0}^2 t_0 - {q_1}^2 t}{2(t_0 + t)} \qquad (9)$$

and for short times $t_0 \gg t$ we find, expanding eq 9 in t and keeping linear terms only

$${q_{max}}^2 \approx \frac{1}{2}\left({q_0}^2 - ({q_0}^2 + {q_1}^2)\frac{t}{t_0}\right) \qquad (10)$$

Here $q_0/\sqrt{2}$ is the location of the Cahn peak before the jump. As we see, the location of the peak position given by q_{max} shifts toward smaller q wavevectors as obtained in experiments. The explanation of the phenomenon is very simple. We have in the Cahn regime one dominant wavevector $q_0/\sqrt{2}$, and the diffusion process first eliminates modes with large wavevectors after the temperature jump. Therefore, the modes with large q decrease much faster than those with small q, and that is why the location of the peak moves toward smaller wavevectors, indicating a growth of the average size of the mode. The process does not involve the movement of the domain boundaries but pure diffusion across the boundaries and decrease of the average saturation inside the domains.

Such analysis can be also done for the intermediate regime of the spinodal decomposition. During the spinodal decompostion, after the growth of uncoupled modes with one dominant Cahn mode, we enter the intermediate regime where modes become coupled[18,30] and the peak position q_{max} starts to shift toward smaller wavevectors algebraically with time $t^{-\beta}$ with the exponent $\beta = 0.21$. In fact, a detailed analysis[9,31−33] shows that during the growth in this regime the exponent β changes continuously from 0 to 1. The type of mode coupling analysis was done for homopolymer blends by Akcasu et al.[21,22] They analyzed a peak position during the spinodal decomposition and after a jump to higher temperature. They found that the decay, after the jump, should follow the path such that asymptotically $q_{max} \sim t^{-0.5}$ and S_{max} should decay exponentially with time. Such behavior although found in experiments[21] is by no means universal as in different system and temperature regime Holoubek found that the peak position shifts toward zero exponentially rather than algebraically.[26,27]

In Figure 4 we show on a single curve the whole evolution of q_{av} in time starting 50 s (stabilization of the temperature) after the quench to $T_0 = 112$ °C. The final temperature is $T_1 = 121$ °C. A jump from 112 to 121 °C is well marked by the change of slope in q_{av} on a log−log plot. q_{av} has a characteristic minimum, and at longer times it grows. The final value of q_{av} is $\sim 1/\xi$, where ξ is the correlation length of the order of the radius of gyration. It is outside the scale of our linear array of photodiodes, and therefore finally at the end of the process we get noisy data. q_{av} decreases after the jump to 121 °C but not in the same way as q_{max}, i.e., not with the same exponent. After a jump (see change of slope in Figure 4) we find $q_{av} \sim t^{-1.3}$ and $q_{max} \sim t^{-2.5}$. The increase of q_{av} at long t is understandable. Once small domains get dissolved completely, we expect that only large domains of similar sizes survive. They dissolve together, decreasing their size in the process, and thus q_{av} increases.

A Jump to the Metastable Region. In Figure 5 we show the behavior of $S(q,t)$ in the metastable region. The peak position as in the jump to the one-phase region

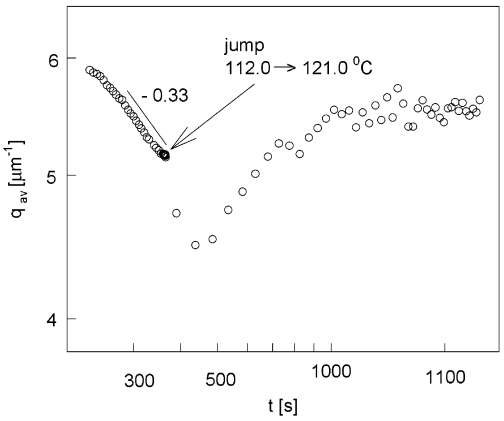

Figure 4. Average wavevector (eq 7) as a function of time for the quench/jump process shown in Figures 2 and 3. The initial temperature is $T_0 = 112$ °C (Figure 2), and the jump to temperature $T_1 = 121$ °C (Figure 3) is clearly marked by the abrupt change of slope. A characteristic minimum is clearly visible. At late times q_{av} reaches a noise level. Each point is the average over 50 experimental points (for clarity and for the reduction of the noise) taken every 0.5 s after the jump.

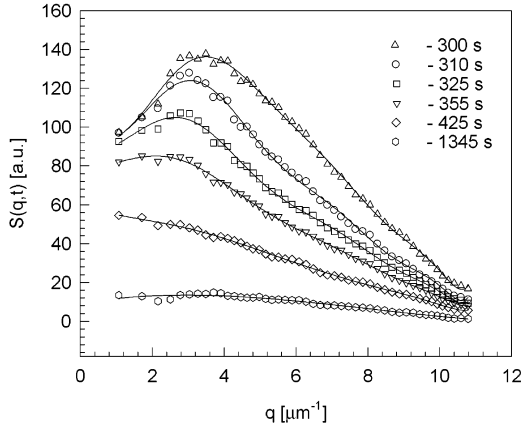

Figure 5. Scattering intensity, $S(q,t)$, after a temperature jump from $T_0 = 112$ °C to the metastable region $T_1 = 119$ °C above the spinodal but below the binodal, as a function of the wavevector q for different times. The peak decreases (indicating the decrease of the saturation of the domains) and its location shifts toward smaller wavevectors, indicating the increase of the average size of the PS-rich and PMPS-rich domains following a global disappearance of small domains. This is a process of partial mixing; i.e., the domains get dissolved, but later on they start to grow again as shown in Figure 6.

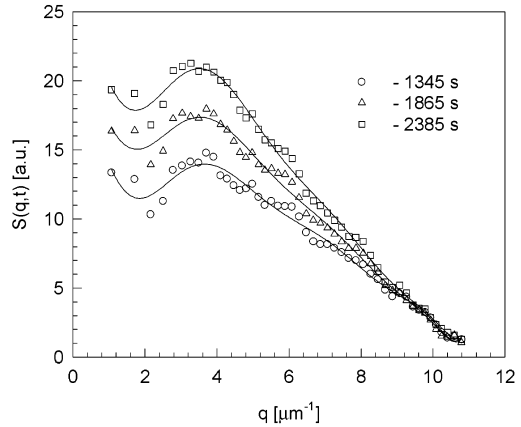

Figure 6. Further evolution of the scattering intensity, $S(q,t)$ (shown in Figure 5), in the metastable region ($T_1 = 119$ °C). The peak shown in Figure 5 reaches a minimum and starts to grow again, because a completely mixed state is not globally stable in the metastable region. The peak increases (domains saturate again), but its location hardly changes. In fact, only in the average wavevector we can see clearly a very slow shift toward smaller wavevectors (Figure 7). This process of demixing follows the process of partial mixing shown in Figure 5. Please note that the peak starts at a different location than the one shown in Figure 5 (see also Figure 7).

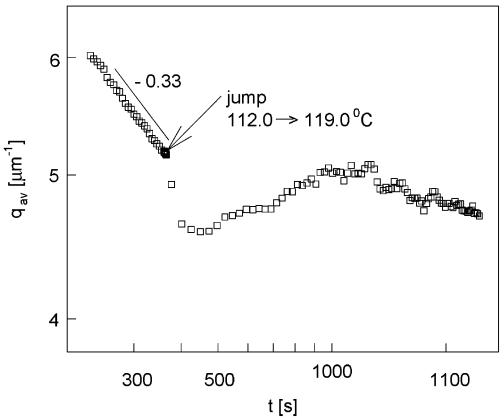

Figure 7. Average wavevector (eq 7) as a function of time for the quench/jump process shown in Figures 2, 5, and 6. The initial temperature is $T_0 = 112$ °C (Figure 2), and the jump to temperature $T_1 = 119$ °C (Figure 5) is clearly marked by the abrupt change of slope. The characteristic minimum and maximum are clearly visible. A decrease of q_{av} at longer times marks clearly a difference between a jump to the one-phase and metastable region (see Figure 4). Each point is the average over 50 experimental points (for clarity and for the reduction of the noise) taken every 0.5 s after the jump.

moves toward smaller wavevectors, but its behavior is slightly different from the previous case. First of all, in the one-phase region the peak decreases completely, whereas in the metastable region it does not. Next after some time the scattering intensity starts to grow again, whereas in the one-phase region it does not. In Figure 6 we show $S(q,t)$ as it increases again. The differences are clearly seen if we plot q_{av} vs time t (log−log scale) as shown in Figure 7. The initial decrease after a quench is shown as in the previous case of the one-phase region, since the initial quench has been done to the same temperature. After a jump to the metastable region, the average wavevector initially decreases (at $T_1 = 119$ °C) as $t^{-1.1}$, attains a minimum, and grows. It reaches a maximum and starts to decreases again, and *this is a main difference between the jump to one-phase and metastable region*. In the one-phase region the maximum in q_{av} is absent. The later growth of q_{av} is very slow and is practically not visible for q_{max} (see Figure 6).

Thus, there are three different regimes in the evolution of $S(q,t)$. After a temperature quench the peak position shifts toward small wavevectors and the peak increases; next, after a temperature jump the peak decreases and shifts quickly toward small wavevectors. The location of the peak reaches a minimum as a function of time. Next, the peak starts to shifts toward *larger* wavevectors but hardly grows. And finally, it starts to grow again with the position which practically does not change. Only q_{av} moves slowly toward small wavevectors. This growth is much slower than the growth observed directly after the quench.

What is surprising in this observation is the fact that the intensity drops down in the metastable region. The size of the domains is few micrometers and is far bigger

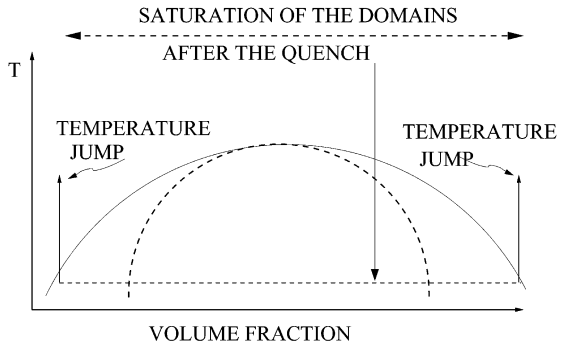

Figure 8. Schematic picture of the general idea which explains the partial mixing phenomenon. In the coarsening process shown in Figure 2 for $S(q,t)$, the domains saturate and the average volume fraction inside domains approach that on the binodal curve. When at this point we make a temperature jump we find that from the point of view of the saturated domains we are in a one-phase region. It means that in order to stabilize a nonuniform distribution of the homopolymers the domains have to dissolve a little to get back on the binodal curve (see also Figure 1).

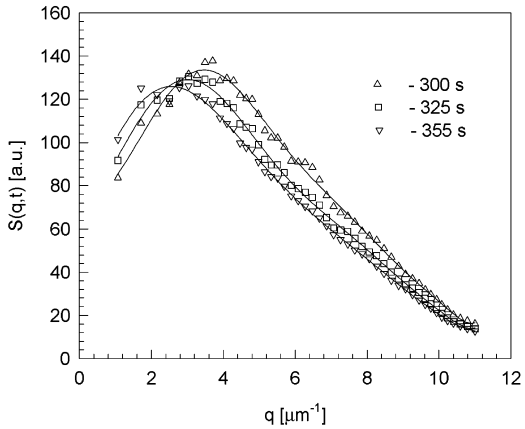

Figure 9. Scattering intensity, $S(q,t)$, after a temperature jump from $T_0 = 112$ °C to the unstable region $T_1 = 116.25$ °C below the spinodal but above T_0, as a function of the wavevector q for three times. The peak intensity decreases a little (indicating the decrease of the saturation of the domains), and its location shifts toward smaller wavevectors. After the initial decrease the peak starts to grow again very slowly as shown in Figure 10. Closer to the temperature T_0 at temperature $T_1 = 115.75$ °C this decrease would be hardly visible.

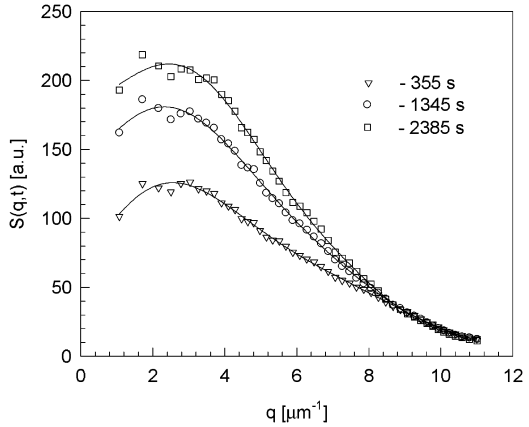

Figure 10. Growth of the scattering intensity, $S(q,t)$, after the initial decrease period (Figure 9) in the unstable region at $T_1 = 116.25$ °C below the spinodal but above T_0, as a function of the wavevector q for three times. The peak increases (indicating the increase of the saturation of the domains), but its location hardly changes.

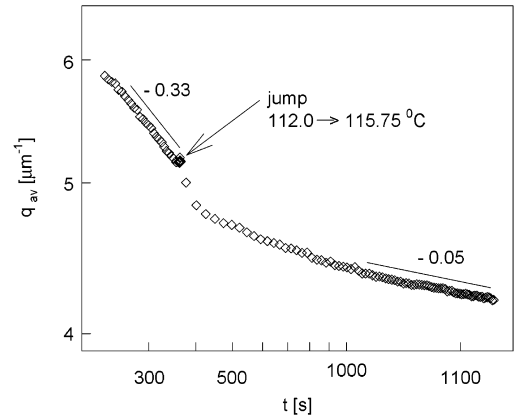

Figure 11. Average wavevector (eq 7) as a function of time for the quench/jump process. The initial temperature is $T_0 = 112$ °C (Figure 2), and the jump to temperature $T_1 = 115.75$ °C below the spinodal is marked by the slight change of slope. The characteristic minimum, which was clearly visible in the one-phase and metastable region, disappears in the unstable region (see Figures 4 and 7). Each point is the average over 50 experimental points (for clarity and for the reduction of the noise) taken every 0.5 s after the jump.

than the critical nucleus. Therefore, we would expect that the intensity should increase after the temperature jump, yet it initially decreases. One of the explanations would be as follows: Lets suppose that the domains are saturated, i.e., that the value of the volume fraction inside the domains is almost that at the coexistence (binodal curve). Since the domains are quite saturated, then when we make a jump to any temperature, we are practically outside the binodal in a one-phase region, at least from the point of view of the local volume fraction of the homopolymers inside domains (shown schematically in Figure 8). The dashed horizontal line shows schematically the change of the average volume fraction inside the domains. As can be seen, the final average volume fraction is very close to the volume fraction at coexistence (at the binodal), and that is why we always see the decay of the scattered intensity after a temperature jump. This explanation is certainly simplified but nonetheless contains the basic physical ingredients.

A Jump to the Unstable Region. One should expect according to the explanation shown in Figure 8 that also a jump into the unstable region should result in the initial decay of the scattering intensity. In Figure 9 we show the decay of $S(q,t)$ after a jump to the unstable region. As we see, the peak decreases a little and the position of the maximum shifts a lot after a jump (as $t^{-0.68}$). In fact, for lower temperatures (closer to T_0) this decrease would be hardly visible in $S(q,t)$, and only after integration over the whole q range (see eq 6) would we see the decrease of the scattering intensity also in the unstable region. Next, $S(q,t)$ very quickly starts to grow again (Figure 10) with a peak which hardly changes its position. Nonetheless, the average wavevector very slowly shifts toward 0 (as $t^{-0.05}$). The characteristic minimum in the average wavevector disappears (Figure 11), and this is the main difference in q_{av} between *metastable and unstable regions*. We have shown here the behavior of $S(q,t)$ for $T_1 = 116.25$ °C and q_{av} for a temperature further from the spinodal at $T_1 = 115.75$ °C to present in the best way the main features of the partial mixing in the unstable region. (The peak hardly changed its shape at 115.75 °C.) q_{av} monotonically decreases toward zero with a slight change of the slope after the jump. In fact, on the basis of the behavior of

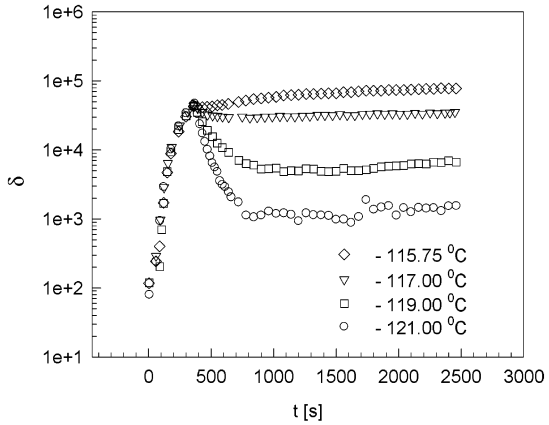

Figure 12. Integrated intensity $\delta = \int dq\, S(q,t)$ as a function of time for various temperatures of the jump. The initial growth of δ shown in the figure is for $T_0 = 112$ °C (Figure 2). The jump to a higher temperature is marked by the maximum of δ. The decay of δ after a jump is exponential in time with a characteristic decay time τ, which goes to infinity as we approach T_0. In the metastable region and below the spinodal we see a clear minimum of δ. The value of δ at the minimum is shown in Figure 13 as a function of the temperature.

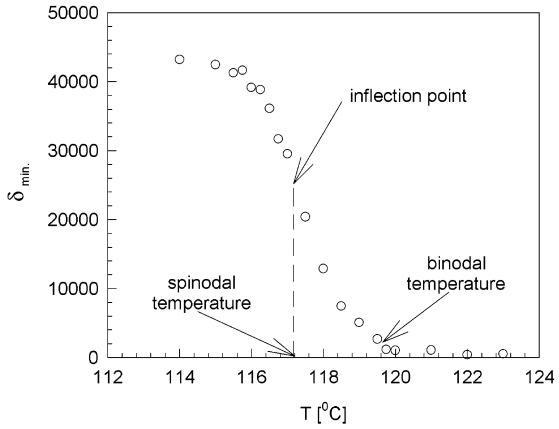

Figure 13. The value of δ (see Figure 12) at the minimum as a function of the temperature. On the basis of δ_{min} we can determine the spinodal temperature T_s and binodal temperature T_b. T_b corresponds to the point where δ_{min} starts to grow as a function of T and T_s to the maximal growth (inflection point of this curve) of $\delta_{min}(T)$.

q_{av}, one can determine the location of the spinodal and binodal. Alternatively, we can use δ (see eq 6) for their determination as we show in the next paragraph.

Determination of the Spinodal and Binodal. In Figure 12 we plot δ as a function of time for different temperatures. As we see, the integrated intensity drops to a very low value in the one-phase region and does not grow later on. In the metastable region it drops down and later on grows again. The characteristic minimum of $\delta(t)$ moves toward longer times as the temperature approaches the spinodal, disappears completely at the spinodal, and reappears below the spinodal. If we plot the value of δ at the minimum (δ_{min}) as a function of temperature, we get Figure 13. The binodal is located at the point where δ_{min} starts to grow, i.e., at $T_b = 119.65 \pm 0.25$ °C. Thus, there are two characteristics of the binodal curve as obtained from δ: the characteristic minimum which is absent in the one-phase region and the visible growth of δ_{min} as a function of temperature below the binodal curve. The spinodal temperature is, on the other hand, determined by the inflection point on the δ_{min} vs temperature plot (i.e., the

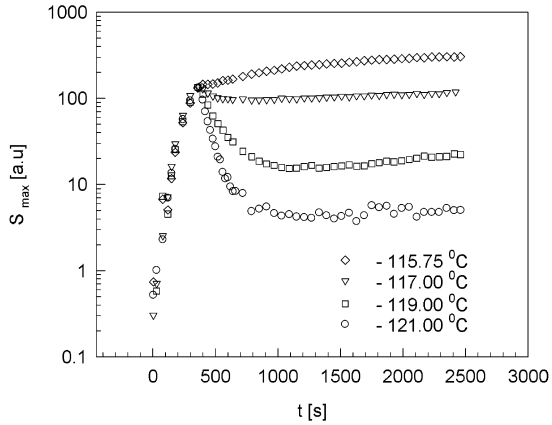

Figure 14. The value of the maximum of the scattering intensity S_{max} as a function of time t for various temperatures. Please compare with a plot of the integrated intensity $\delta = \int dq\, S(q,t)$ (Figure 12). Both quantities provide the same information; only the data for S_{max} are usually more noisy.

point of the fastest changes of δ_{min} with temperature). We find $T_s = 117.25 \pm 0.25$ °C. The latter result was in fact first obtained in computer simulations, and on this basis the inflection point was used as a signature of the spinodal. By the way we show in Figure 14 S_{max} as a function of time for different temperatures. Its qualitative behavior is the same as that of δ.

The average wavevector q_{av} provides even more convenient way for the determination of the binodal and spinodal. In Figure 15 we show q_{av} for different temperatures close to the binodal. Near the binodal the data at long times are noisy, whereas below the binodal we observe a very clear maximum on the curve for longer times. From this figure we find the binodal temperature at $T_b = 119.65 \pm 0.15$ °C. The location of the spinodal temperature is related to the characteristic minimum of q_{av}, which disappears at the spinodal and below the spinodal as seen in Figure 16 and Figure 11. The spinodal temperature is thus $T_s = 117.25 \pm 0.25$ °C. Additionally, we have performed the measurements for the 50/50% composition. This mixture was kept for 15 min in the unstable state at $T_0 = 112$ °C. (For longer times the peak shifts too close to the small wavevectors and after the jump disappears from the photodiodes.) The results for the jump close to the spinodal (below and above) are shown in Figure 17. On this basis we have determined the spinodal temperature at $T_s = 122.40$ °C. Similarly (as done in Figure 15), we have determined for 50/50% composition the binodal temperature at $T_b = 123.15$ °C. To see the process at very long times (not accessible in light scattering due to the small angle cutoff and disappearance of the peak at small angles), we have kept the 50/50% mixture for 270 min at $T_0 = 112$ °C and performed optical measurements using an Optical Microscopy Nikon Eclipse E400. The observation has been done under the magnification of 750×, but the photographs were taken with the magnification of 250×. The samples were placed on the heating stage, under the microscope, with the 0.01 deg control of the temperature, the same as in the scattering experiment. We have made the temperature jump to the metastable region ($T_1 = 123$ °C) and below the spinodal to $T_1 = 121$ °C. The photographs are shown in Figure 18. The large difference in the number of domains left after the temperature jump to the unstable and metastable region is a clear indication that the spinodal strongly affects partial mixing. Please note that the

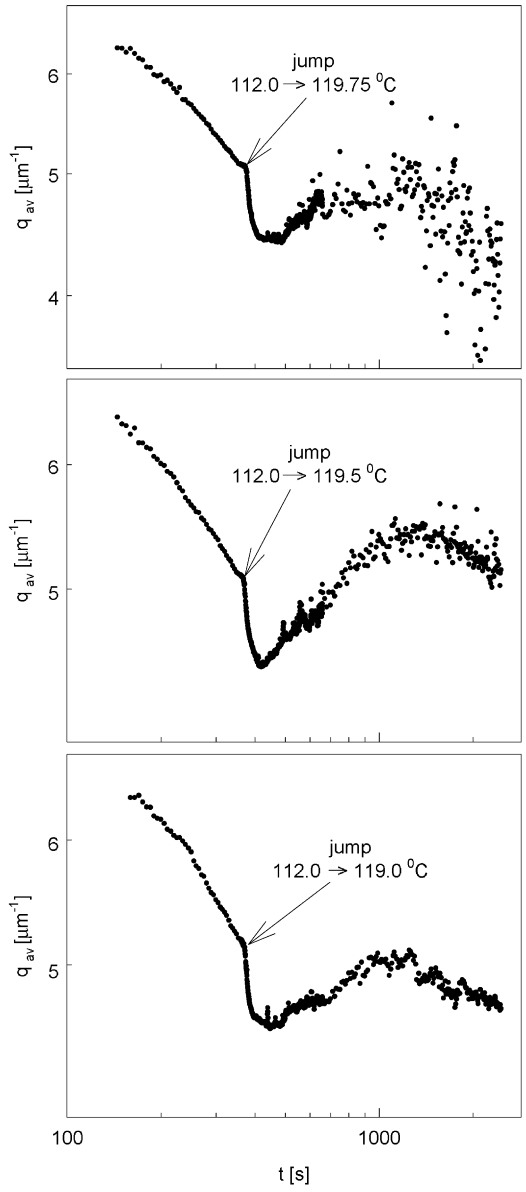

Figure 15. Average wavevector (eq 7) as a function of time for the quench/jump process, for temperatures close to the binodal for the 60/40% of PS/PMPS. A characteristic maximum develops just below the binodal. Above the binodal q_{av} reaches a noise level clearly shown in this figure. On this basis the binodal can be located at $T_b = 119.65$ °C. Please note that here we have shown all the data with each point taken every 5 s for a quench and every 0.5 s after the quench, whereas in Figures 4, 7, and 11 each point is the average over 50 experimental points (for clarity and for the reduction of the noise in the case of Figure 4).

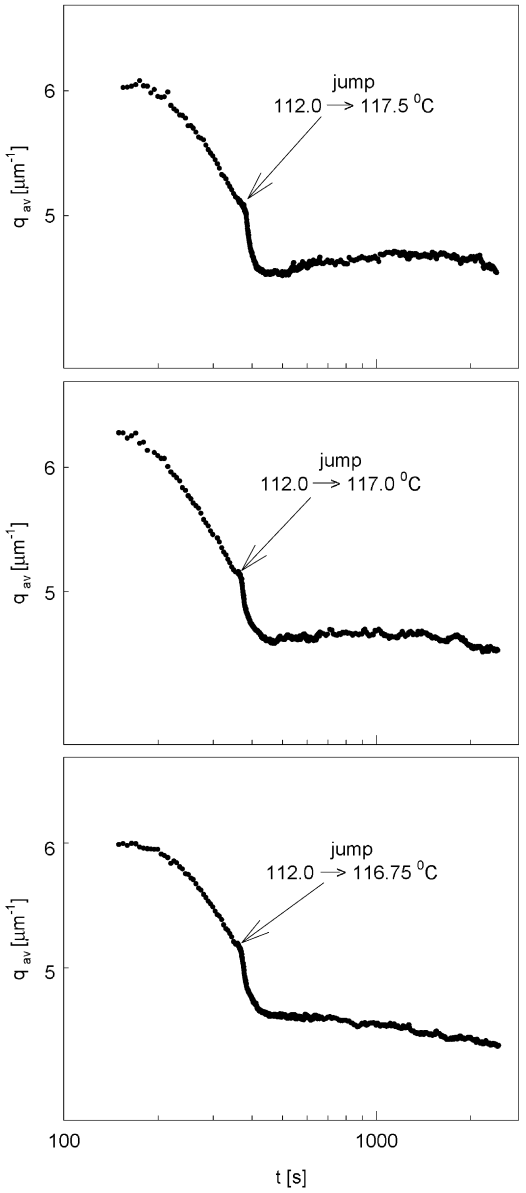

Figure 16. Average wavevector (eq 7) as a function of time for the quench/jump process, for temperatures close to the spinodal for the 60/40% of PS/PMPS. A characteristic minimum develops just above the spinodal. On this basis the spinodal can be located, here at $T_s = 117.25$ °C (see also Figure 17 for the 50/50% mixture). Below the spinodal q_{av} decays monotonically with time after the temperature jump. See also the legend in Figure 15.

optical measurements are complementary to the scattering experiments. In scattering experiments the largest domains that we can possibly measure on the array of photodiodes are of the size of 5 μm or less, whereas in the optical measurements we can easily study the domains bigger than 5 μm. (Smaller domains are also visible but are not easy to use for e.g. size measurements.) Please note that the growth in the unstable region is much slower after the jump (compare the growth after 30 min and 60 min after the jump to $T_1 =$ 121 °C).

The great advantage of our methods for the determination of the binodal and spinodal temperature is its accuracy and convenience. It took only 2 days to obtain both temperatures for a given composition of our sample. Using the standard method, it would be less accurate and would take at least a week. We have called our method JSS (jump spinodal specification).

4. Computer Simulations

To check that the JSS method is not specific to the polymers used in our studies, but is generic, we have performed computer simulations for the generic model of polymer mixtures: the Flory−Huggins−de Gennes model with the Langevin dynamics. This model has been already studied in the context of late stage scaling in spinodal decomposition in polymer mixtures[34,35] and morphological changes during spinodal decomposition.[36,37] Here we will use this model to see the process of mixing in homopolymer blends after the temperature

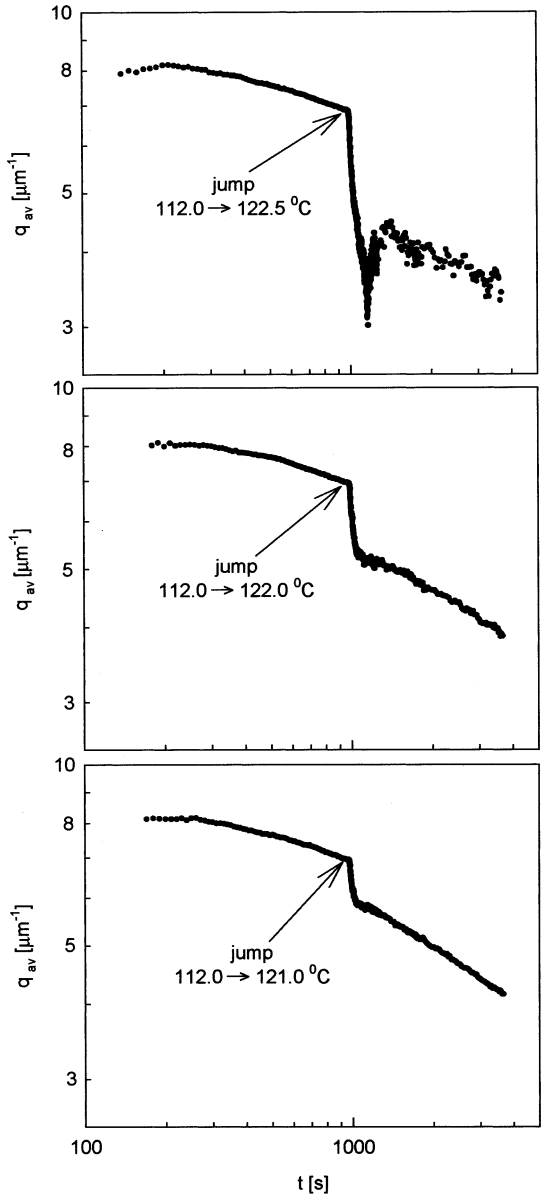

Figure 17. Average wavevector (eq 7) as a function of time for the quench/jump process, for temperatures close to the spinodal for the 50/50% of PS/PMPS. A characteristic minimum develops just above the spinodal. On this basis the spinodal can be located, here at T_s = 122.25 °C. Below the spinodal q_{av} decays monotonically with time after the temperature jump. We have also located the binodal at T_b = 123.15 °C. It seems to us that the depth of the minimum in the metastable region may strongly depend on the proximity of the binodal and spinodal curves (see Figures 16 and 21). Please note that a rapid decrease of q_{av} in the spinodal region which lasts for about 50 s is due to the stabilization of temperature.

jump to the homogeneous, metastable and unstable region.

Below we describe in detail the model. We consider a homopolymers blend (AB) that consists of the molecules with the same indices of polymerization, N, and the same Kuhn segment lengths, σ. The average volume fraction of the A component in the system is ϕ_0, and the state of the system is described by the local volume fraction of the component A, $\phi(\mathbf{r})$, at all points, $\mathbf{r}$, of the system. The phenomenological mesoscopic Langevin-type dynamic equation that relates a temporal change of $\phi(\mathbf{r})$ to a local current of A component, J, is simply a continuity equation,[2]

$$\frac{\partial\phi(\mathbf{r},t)}{\partial t} = -\nabla J + \eta(\mathbf{r},t) \tag{11}$$

where the stochastic term $\eta(\mathbf{r},t)$ has been added in order to model the thermal noise in the system.[18−20] In the limit of the infinite viscosity, we can neglect the hydrodynamic flux contribution $\phi(\mathbf{r})\mathbf{v}(\mathbf{r})$ to the local current J ($\mathbf{v}(\mathbf{r})$ is a local velocity). In this case, the transport in the system is governed by the difference of the chemical potential, and one can postulate a linear relation between the local current and the gradient of the local chemical potential difference $\mu(\mathbf{r})$,[1,3]

$$J(\mathbf{r}) = -\int \frac{\Lambda(\mathbf{r}-\mathbf{r}')}{k_B T}\,\nabla'\mu(\mathbf{r}')\,\mathrm{d}\mathbf{r} \tag{12}$$

The local chemical potential difference $\mu(\mathbf{r})$ is given by the functional derivative of a coarse-grained free energy functional $F[\phi]$,

$$\mu(\mathbf{r}) = \frac{\delta F[\phi]}{\delta\phi(\mathbf{r})} \tag{13}$$

The minimal length scale at which we shall describe the phase separation phenomena is about the size of a single polymer molecule. At this length scale we can approximate the nonlocal Onsager coefficient $\Lambda(\mathbf{r}-\mathbf{r}')$ by the following expression:

$$\Lambda(\mathbf{r}-\mathbf{r}') \simeq ND\phi(1-\phi)\,\delta(\mathbf{r}-\mathbf{r}') \tag{14}$$

where D is the self-diffusion coefficient of the polymer chains. Then we can take, consequently, the coarse-grained free energy functional $F[\phi]$ in the Flory−Huggins−de Gennes form:

$$F[\phi(\mathbf{r})]/k_B T = \int \mathrm{d}^3 r\left[f(\phi(\mathbf{r})) + \frac{\sigma^2}{36\phi(1-\phi)}(\nabla\phi(\mathbf{r}))^2\right] \tag{15}$$

where f is the usual Flory−Huggins free energy:

$$f(\phi(\mathbf{r})) = \frac{1}{N}\{\phi\ln(\phi) + (1-\phi)\ln(1-\phi)\} + \chi\phi(1-\phi) \tag{16}$$

We introduce the following rescaled variables:

$$\mathbf{x} = \frac{(\chi-\chi_s)^{1/2}}{\sigma}\,\mathbf{r} \tag{17}$$

$$\tau = \frac{D(\chi-\chi_s)^2}{\chi_s\sigma^2}\,t \tag{18}$$

Here χ is the Flory−Huggins interaction parameter, $\chi_s = 1/(2N\phi_0(1-\phi_0))$ and $\chi_c = 2/N$ are the values of χ at the spinodal and the critical point, respectively. The final equation to be solved numerically is written in the rescaled variables as (assuming constant mobility)[34]

$$\frac{\partial\phi(\mathbf{x},\tau)}{\partial t} = \frac{1}{2}\nabla^2\left(\frac{\chi_c}{2(\chi-\chi_c)}\ln\frac{\phi}{1-\phi} - \frac{2\chi\phi}{\chi-\chi_c} - \frac{1}{18\phi(1-\phi)}\nabla^2\phi + \frac{1-2\phi}{36\phi^2(1-\phi)^2}(\nabla\phi)^2\right) + \sqrt{\epsilon}\zeta(\mathbf{x},\tau) \tag{19}$$

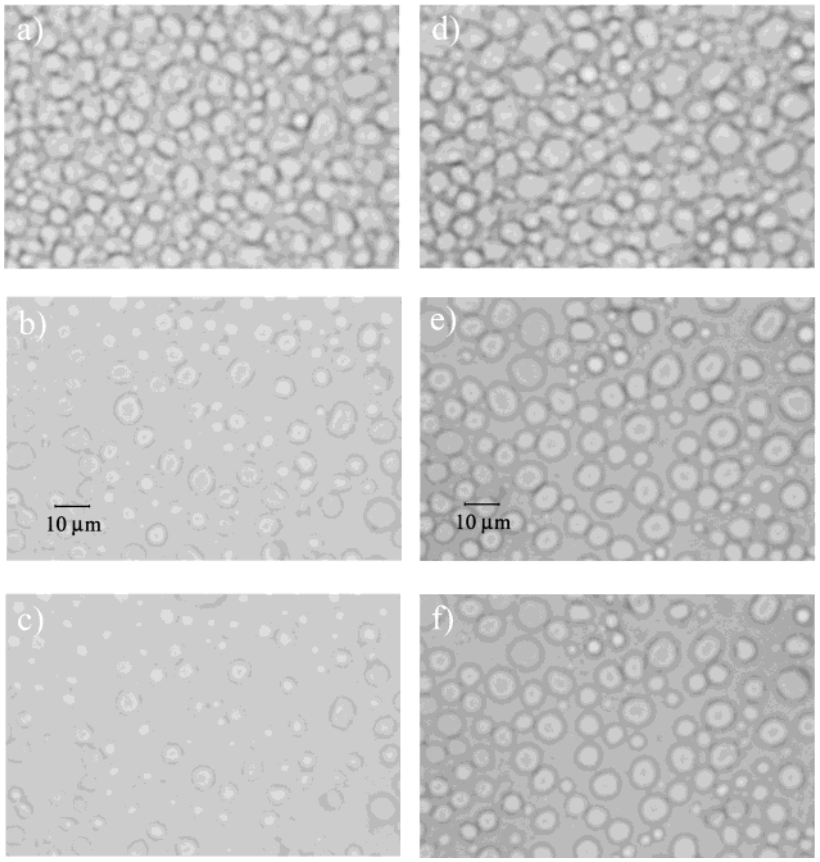

Figure 18. Observation of the large domains in the optical microscopy **(**a**). (**d**)** shows the morphology of the 50/50% of PS/PMPS system at temperature $T_0 = 112$ °C after 270 min in the unstable region. The spinodal has been located at $T_s = 122.25$ °C and the binodal at $T_b = 123.15$ °C. We make a temperature jump to the metastable region to $T_1 = 123$ °C **(**b**)** ((30 min after the jump) **(**c**)** (60 min after the jump)) and to the unstable region to $T_1 = 121$ °C **(**e**)** (also 30 min after the jump) and **(**f**)** (60 min after the jump). First of all, we see the huge difference in the number of the domains after the jump to the metastable and unstable region compare **(**c**)** ($T_1 = 123$ °C) and **(**f**)** ($T_1 = 121$ °C). Moreover, if we compare **(**e**)** and **(**f**),** we see that the growth after the jump is very slow; also Figure 11, i.e., the change of the wavevector (slopes) and Figure 10, i.e., the growth of the peak. Both observations made under the microscope support our conjecture that spinodal curve strongly affects the demixing process.

where the noise term $\zeta(\mathbf{x},\tau)$ should satisfy the fluctuation−dissipation theorem (FDT),

$$\langle \zeta(\mathbf{x},\tau)\zeta(\mathbf{x}',\tau')\rangle = -\nabla^2\delta(\mathbf{x}-\mathbf{x}')\,\delta(\tau-\tau') \qquad (20)$$

and the noise intensity $\epsilon = \sqrt{(\chi-\chi_s)}$.

To solve numerically eq 19, we use the first-order Euler scheme,

$$\phi(\bar{\mathbf{x}},\tau+\Delta\tau) = \phi(\bar{\mathbf{x}},\tau) + \Delta\tau\,\frac{\partial\phi(\bar{\mathbf{x}},\tau)}{\partial\tau} + \bar{\zeta}(\bar{\mathbf{x}}) \qquad (21)$$

where $\bar{\mathbf{x}} = \Delta x[i, j, k]$, $i, j, k = 1,..., L$ is a position vector at the lattice, Δx is a lattice spacing (mesh size), and $\Delta\tau$ is a time step. In the last equation we have written explicitly the rescaled noise term $\bar{\zeta}(\bar{\mathbf{x}})$, which has to be generated at each time step and at each lattice site in accordance with the FDT (eq 20). In practice, to generate the noise in accordance with eq 20, we, following the ideas of Puri and Oono,[38] introduce the additional vector white noise $\bar{\xi}$ with the Gaussian components, which satisfies the following relation:

$$\langle \xi_i(\mathbf{x},\tau)\,\xi_j(\mathbf{x}',\tau')\rangle = \delta_{i,j}\delta(\mathbf{x}-\mathbf{x}')\,\delta(\tau-\tau') \qquad (22)$$

If we now relate our noise variable ζ to ξ as

$$\zeta(\mathbf{x},\tau) = \vec{\nabla}\xi(\mathbf{x},\tau) \qquad (23)$$

the FDT (20) will be satisfied. The white noise components are generated from the Gaussian distribution independently at each lattice site. Finally, the noise contribution to the discrete eq 21 reads

$$\bar{\zeta} = \sqrt{\frac{\Delta\tau}{(\Delta x)^3}}(\chi-\chi_s)^{1/4}\xi \qquad (24)$$

i.e., is dependent on the discretization.[39,40]

We have solved the eq 19 numerically for the polybutadiene−deuterated polybutadiene blend characterized by the average volume fraction $\phi = 0.6$. For this system the Flory−Huggins parameter $\chi = 0.326/T - 0.00023$ has been determined experimentally.[41] The critical temperature for this system is $T_c = 62$ °C, and the polymerization index is $N \approx 4500$. The value of the FH parameter at the critical temperature T_c is $\chi_c = 2/N$, $\Lambda = ND\phi_0(1-\phi_0)$, where D is the diffusion constant, which is inversely proportional to N^2, and ϕ_0 is the average composition in the system. The spinodal and the coexistence (binodal) curves are given by the conditions $\chi_s = 1/(2N\phi_0(1-\phi_0))$ and $\chi_b = -\ln(\phi_0/(1-\phi_0))/N(1-2\phi_0)$, respectively. The corresponding spinodal and binodal temperatures, calculated from χ_s and χ_b for $\phi_0 = 0.6$, are $T_s = 51.67$ °C and $T_b = 58.54$ °C.

We have performed the simulations for exactly the same process as studied in our experiment (see Figure 1). The system was first quenched to the temperature

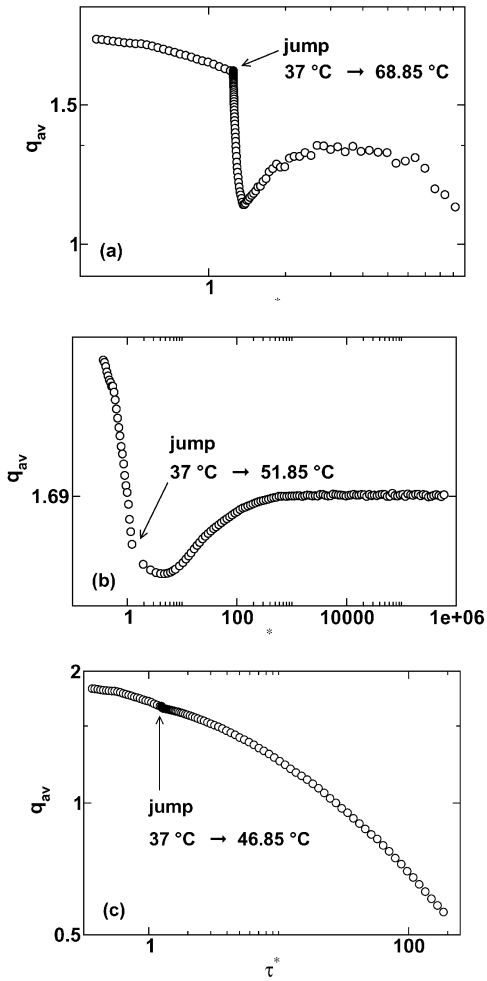

Figure 19. Average wavevector (eq 7) as a function of time for the quench/jump process, for temperatures close to the spinodal obtained in the computer simulations of the 60/40% of hPb/dPb mixture. We quenched the system first to $T_0 = 37$ °C and kept it at this temperature for a short time $\tau = 1.25$ (domains were not saturated). A characteristic minimum develops just above the spinodal. Below the spinodal q_{av} decays monotonically with time after the temperature jump. On this basis the spinodal can be located, here at $T_s = 51.67 \pm 0.18$ °C, which agrees perfectly with the spinodal obtained in the Flory−Huggins−de Gennes model ($T_s = 51.67$ °C). We have also located the binodal at $T_b = 58.54 \pm 0.2$ °C in the same way as in the experiment. The vaule of T_b is the same as obtained from the Flory−Huggins−de Gennes model ($T_b = 58.54$ °C). To show all the functions in the same time scale, the dimensionless quantity τ has been replaced by the relative time τ^* defined as $\tau^* = (\chi_1 - \chi_s)^{-2}(\chi_0 - \chi_s)^2\tau$, where χ_0 and χ_1 are respectively the FH parameter corresponding to the quench, T_0, and the jump, T_1, temperatures.

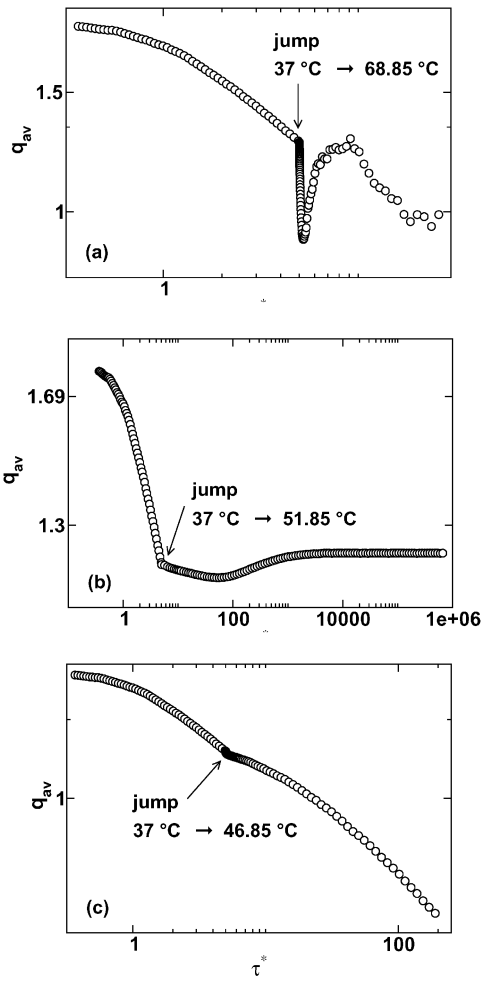

Figure 20. Same legend as in Figure 19. Here we have only kept the mixture at $T_0 = 37$ °C for a long time $\tau = 5$. We have observed a saturation of the domains; i.e., the volume fractions of the polymers were close to their values at coexistence. A characteristic minimum which develops just above the spinodal does not depend on the time the mixture was kept in the unstable region (compare Figures 19 and 20), and this shows that in a jump spinodal specification method this time is irrelevant and can be adjusted at will in the experiment.

$T_0 = 37$ °C below the spinodal temperature and allowed to demix for two different times $\tau_s = 1.25$ (short time, domains are not saturated, and we do not observe scaling) and $\tau_s = 5$ (long time, where the domains are saturated, and we enter the scaling regime) and then heated to different temperatures T_1 either above or below the spinodal. The scaling regime with the growth exponent $^1/_3$ (see refs 34 and 35) is observed in our simulations; we run them for $\tau > 40$. The results for the determination of the spinodal do not depend on the time the mixture spends after the quench at $T_0 = 37$ °C. We have carried out the simulations on a cubic ($L^3 = 64^3$) lattice using the first-order Euler integration scheme with the mesh size $\Delta x = 0.5$ and the time step $\Delta\tau = 0.0005$. The initial conditions were chosen from the uniform distribution form [$\phi_0 - 0.05$, $\phi_0 + 0.05$]. Before the quench was made, the system was allowed to relax at the temperature 107 °C for a long time. All results have been averaged over a few different initial noise realizations. To show all the functions in the same time scale, the dimensionless quantity τ has been replaced by the relative time τ^* defined as $\tau^* = (\chi_1 - \chi_s)^{-2}(\chi_0 - \chi_s)^2\tau$, where χ_0 and χ_1 are respectively the FH parameter corresponding to the quench, T_0, and the jump, T_1, temperatures.

In Figure 19 we have shown the average wavevector q_{av} as a function of time after the temperature jump to the unstable and metastable region for $\tau_s = 1.25$ (time spent in the unstable region at $T_0 = 37$ °C). The domains are not saturated for this short time. In Figure 20 the same plots are shown but for $\tau_s = 5$. (For this long time the domains are saturated at their coexistence value.) We find the same features of the process as in the experimental study irrespective of whether we kept the mixture in the unstable regime for a short time (with no saturation inside the domains) or for a long time where the domains are saturated; i.e., the volume fraction inside the domains corresponds to the their value at coexistence. It also shows that the JSS method

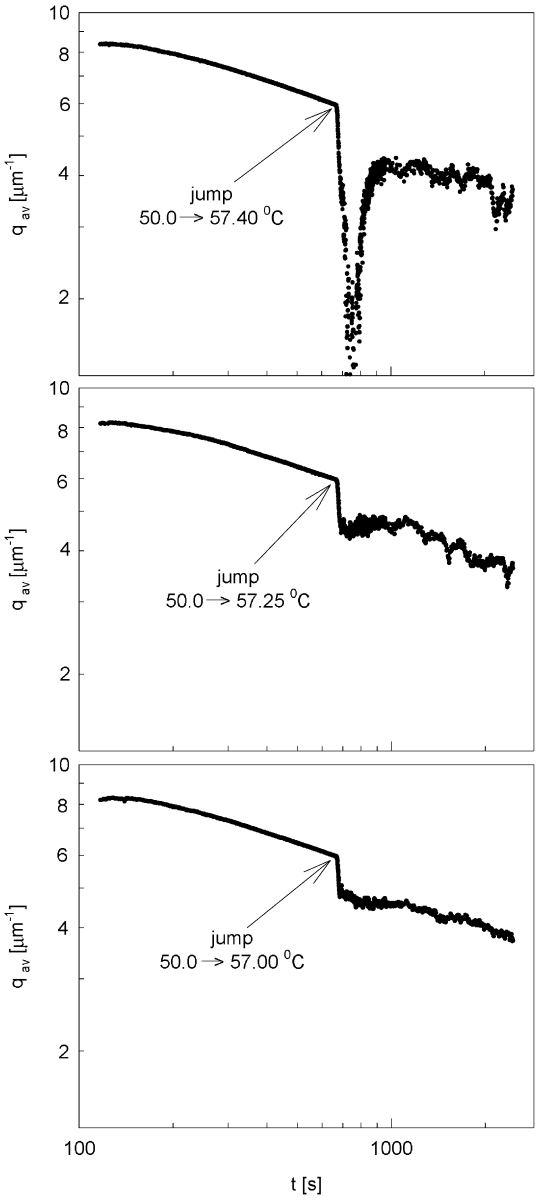

Figure 21. Average wavevector (eq 7) as a function of time for the quench/jump process for the low molecular weight substance 4-cyano-4′-*n*-octylbiphenyl (8CB) mixed with PS in 70/30 wt % for the jump close to the spinodal. The spinodal in this system has been located at $T_s = 57.25$ °C, and we have also located (similarly as shown in Figure 15) the binodal at $T_b = 58$ °C. Please note the same characteristic minimum in q_{av} which was found in three other systems studied (Figures 16−19). A rapid decay of q_{av} after the jump is here due to the stabilization of the temperature. It is absent in computer simulations (see Figures 19 and 20). It shows that the jump spinodal specification method is can be also applied to polymers in low molecular weight solvents.

is generic and not restricted to any specific polymer mixture.

5. Concluding Remarks

In the present paper we have proposed a new method for the determination of the spinodal and binodal temperatures. The methods used so far were based on the observation of the development of the nonuniform states after the temperature quenches below the binodal. Our method is based on the characteristic behavior of q_{av} (eq 7) (and also δ (eq 6)) after the temperature jump. Therefore, it is the observation of the decay of nonuniform states in homopolymer blends, developed after the temperature quench, which gives the location of both temperatures. The method (jump spinodal specification, JSS) is very efficient and very convenient. Needless to say, the JSS method is much faster than the previous methods. The method consists of the following steps (Figure 1): quench well below the spinodal → demix at this temperature for a couple of minutes → the temperature jump to a higher temperature and observation of the behavior of q_{av} (eq 7). Below the spinodal q_{av} monotonically decreases with time (e.g., Figures 11 and 16). Between the spinodal and binodal in the metastable region q_{av} has a clear minimum and maximum (Figures 7, 11, and 15). And finally above the binodal there is a minimum followed by the noise level without a maximum (Figures 15 and 4). The JSS method, which is described in this paper, has been also checked in computer simulations of the polybutadiene/deuterated polybutadiene, showing its generic nature. Finally, we would like to show how JSS method works in the case of low molecular weight solvent and polymer. We have done some very preliminary studies of the 4-cyano-4′-*n*-octylbiphenyl (8CB) mixed with PS in 70/30 wt %. In Figure 21 we show the results for q_{av} for the scattering near the spinodal. The spinodal in this system has been located at $T_s = 57.25$ °C, and we have also located (similarly as shown in Figure 15) the binodal at $T_b = 58$ °C.

By the way we have shown how the mixing process occurs in homopolymer blends in the one-phase, metastable and unstable region. It was suprising at first to observe that even in the metastable and unstable region we observe a partial mixing of the components. The further analysis of the process will be helpful in a better understanding of the mixing and demixing of homopolymers and its applications.

Acknowledgment. This work has been supported by the KBN under Grants 5 P03B09421 and 2P03B00923. R.H. acknowledges with appreciation the stipendship from the French Ministry of Education.

References and Notes

(1) de Gennes, P. G. *J. Chem. Phys.* **1980**, *72*, 4756.
(2) Pincus, P. *J. Chem. Phys.* **1980**, *75*, 1996.
(3) Binder, K. *J. Chem. Phys.* **1983**, *79*, 6387.
(4) Wiltzius, P.; Bates, F. S.; Heffner, W. R. *Phys. Rev. Lett.* **1988**, *60*, 1538.
(5) Bates, F. S.; Wiltzius, P. *J. Chem. Phys.* **1989**, *91* 3258.
(6) Cumming, A.; Wiltzius, P.; Bates, F. S. *Phys. Rev. Lett.* **1990**, *65*, 863.
(7) Cumming, A.; Wiltzius, P.; Bates, F. S.; Rosendale, F. H. *Phys. Rev. A* **1992**, *45*, 885.
(8) Krausch, G.; Dai, C. A.; Kramer, E. J.; Bates, F. S. *Phys. Rev. Lett.* **1993**, *71*, 3669.
(9) Hashimoto, T. *Phase Transitions* **1988**, *12*, 47.
(10) Hashimoto, T. In *Materials Science and Technology;* Cahn, R. W., Haason P., Kramer, E. J., Eds.; VCH: Weinheim, 1993; Vol. 12, pp 252−300.
(11) Hashimoto, T.; Itakura, M.; Hasegawa, H. *J. Chem. Phys.* **1986**, *85*, 6118.
(12) Izumitani, T.; Takenaka, M.; Hashimoto, T. *J. Chem. Phys.* **1990**, *92*, 3213.
(13) Jinnai, H.; Koga, T.; Nishikawa, Y.; Hashimoto, T.; Hyde, S. T. *Phys. Rev. Lett.* **1997**, *78*, 2248.
(14) Koga, T.; Jinnai, H.; Hashimoto, T. *Physica A* **1999**, *263*, 369.
(15) Takeno, H.; Iwata, M.; Takenaka, M.; Hashimoto, T. *Macromolecules* **2000**, *33*, 9657.
(16) Jinnai, H.; Yoshida, H.; Kimishima, K.; Funaki, Y.; Hirokawa, Y.; Ribbe, A. E.; Hashimoto, T. *Macromolecules* **2001**, *34*, 5186.
(17) Binder, K. *J. Non-Equilib. Thermodyn.* **1998**, *23*, 1.

(18) Langer, J. S. In *Solids far from Equilibrium;* Godrèche, C., Ed.; Cambridge University Press: Cambridge, 1992.
(19) Gunton, J. D.; San Miguel, M.; Sahni, P. S. In *Phase Transition and Critical Phenomena;* Domb, C., Lebowitz, J. L., Eds.; Academic Press: London, 1983; Vol. 8, pp 267−455.
(20) Bray, A. J. *Adv. Phys.* **1994**, *43*, 357.
(21) Akcasu, A. Z.; Bahar, I.; Erman, B.; Feng, Y.; Han, C. C. *J. Chem. Phys.* **1992**, *97*, 5782.
(22) Akcasu, A. Z.; Klein, R. *Macromolecules* **1993**, *26*, 1429.
(23) Hammouda, B.; Balsara, N. P.; Lefebvre, A. A. *Macromolecules* **1997**, *30*, 5572.
(24) Ermi, B. D.; Karim, A.; Douglas, J. F. *J. Polym. Sci., Part B: Polym. Phys.* **1998**, *36*, 191.
(25) Vailati, A.; Giglio, M. *Nature (London)* **1997**, *390*, 262.
(26) Holoubek, J. *Macromol. Symp.* **2000**, *149*, 119.
(27) Holoubek, J. *Macromol. Symp.*, **2000**, *162*, 307.
(28) Okada, M.; Tao, J.; Nose, T. *Polymer* **2002**, *43*, 329.
(29) Zhou, Z.; Yan, D. *Macromol. Theory Simul.* **1997**, *6*, 597.
(30) Langer, J. S.; Bar-on, M.; Miller, H. D. *Phys. Rev. A* **1975**, *11*, 1417.
(31) Furukawa, H. *Adv. Phys.* **1985**, *34*, 703.
(32) Kawasaki, K.; Ohta, T. *Prog. Theor. Phys.* **1978**, *59*, 362.
(33) Siggia, E. D. *Phys. Rev. A* **1979**, *20*, 595.
(34) Chakrabarti, A.; Toral, R.; Gunton, J. D.; Muthukumar, M. *Phys. Rev. Lett.* **1989**, *63*, 2072.
(35) Brown, G.; Chakrabarti, A. *J. Chem. Phys.* **1993**, *98*, 2451.
(36) Aksimentiev, A.; Moorthi, K.; Hołyst, R. *J. Chem. Phys.* **2000**, *112*, 6049.
(37) Aksimentiev, A.; Fiałkowski, M.; Hołyst, R. *Adv. Chem. Phys.* **2002**, *121*, 143.
(38) Puri, S.; Oono, Y. *Phys. Rev. A* **1988**, *38*, 1542.
(39) van Vlimmeren, B. A. C.; Fraaije, J. G. M. E. *Comput. Phys. Commun.* **1996**, *99*, 21.
(40) Van Kampen N. G. *Stochastic Processes in Physics and Chemistry;* Elsvier Science: Amsterdam, 1992.
(41) Bates, F. S.; Wignall, G. D.; Koehler, W. C. *Phys. Rev. Lett.* **1985**, *55*, 2425. Bates, F. S.; Wignall, G. D. *Macromolecules* **1986**, *19*, 932.

MA020499C